Coordinated Control Strategy of Distributed Energy Resources based Hybrid System for Rural Electrification

Swati Bhamu*‡, T. S. Bhatti*

*Centre for Energy Studies, IIT Delhi

Hauz Khas, New Delhi- 110016, India

(swatibhamu@gmail.com, tsb@ces.iitd.ac.in)

‡Corresponding Author; Ph.D. Research Scholar, CES IIT Delhi

Tel: +91 9873293624, swatibhamu@gmail.com

Received: 14.01.2018 Accepted:14.02.2018

Abstract- A novel active and reactive power control strategy of a wind-biogas based hybrid system for rural electrification (HSRE) has been proposed. The purpose of the model is to provide continuous and reliable power supply to a cluster of villages while maintaining power balance between system components along with regulation of voltage and frequency. A defined amount of power supply is taken from grid and the rest is supplied by a combination of controllable and intermittent sources of energy. The defined grid operation concept is achieved by considering dynamics of system voltage angle as well which cannot be achieved by the usual control techniques for frequency and voltage magnitude. Induction generator (IG) based Wind energy conversion system (WECS) has been chosen as a source for HSRE whose dynamic model for power control has been developed. Since reactive power is required by IG and the load therefore Static synchronous compensator (STATCOM) has been incorporated. For power generation from biogas-genset, synchronous generator has been used which is fitted with electronic speed governor and automatic voltage regulator (AVR). Finally, small signal stability studies have been carried to investigate the dynamic performance of the system for load and input wind power disturbance.

Keywords Hybrid system for rural electrification (HSRE), WECS, SCIG, STATCOM, biogas-genset, defined grid supply system

NOMENCLATURE

P_{WIG}, P_{BSG}, P_G, P_L	Active power output of IG based WECS, biogas, grid and load demand respectively
Q_{WIG}, Q_{BSG}, Q_G, Q_L	Reactive power output of IG based WECS, biogas, grid and load demand respectively
ΔP, ΔQ	Change in corresponding active and reactive power
$V\angle-\theta$, $E_G\angle 0$ and f	System bus voltage, grid voltage, frequency
T_{B1}-T_{B7}	Time constants of electronic speed governor, actuator and engine/generator
T_{AB}, T_B, T_{EB}, T_{FB}, T_{do}'	Time constants of biogas generator field and AVR system
pf_B	Power factor of synchronous generator
PI 1-PI 4	Proportional Integral controllers

1. Introduction

According to the World Bank report about 14.6% of the world population still don't have any access to electricity, mostly belonging to rural areas of developing countries [1]. The total number of unelectrified villages in India was 12,288 and partially electrified was 304,014 as on 31-3-2016 [2]. Even in the areas with electrification there are power cuts of few to considerable number of hours and continuous supply of electricity is still an outreach. Most popular source of rural electrification (RE) has been diesel gensets as they ensure high reliability in providing power but various drawbacks like high fuel cost, pollution etc. makes it an undesirable long-term solution [3]. To provide a reliable and continuous means of power supply for RE, the distributed energy resources such as wind, solar, biomass are integrated with conventional sources also known as hybrid power system(HPS) [4-5]. These hybrid systems can either be grid

connected or standalone. As higher levels of renewable energy sources (RES) are integrated into the grid several problems are identified such as loss of synchronization, flickers, oscillations, voltage collapse, protection failure etc. [6]. Energy storage can help with key integration challenges, but it is also one of the most expensive options [6]. At present the interest is growing in stand-alone or hybrid systems [7]. Amongst the available renewable sources, biogas has proven to be a reliable option which can replace the traditional diesel generators since it is readily available in rural areas from biodegradable waste [8]. Synchronous generators driven by biomass/biogas engine as a prime mover are generally used and in some applications induction generator is used [9-10]. Another popular source of RE is wind energy which has been the fastest growing renewable energy technology [11]. Amongst various electrical machinery technologies used, the squirrel cage induction generator (SCIG) offers the benefit of minimal maintenance, ruggedness, absence of another DC source for excitation, self-protection against short circuits and overloads, high reliability, low cost and is very light in weight. Though they have the disadvantage of needing reactive power for their operation [12]. For fulfilling this continuous and rapid demand of reactive power by SCIG different Flexible AC transmission system (FACTS) devices are available in the market [13]. Amongst various FACTS devices available, static VAR compensator (SVC), switched capacitors and static synchronous compensator(STATCOM) can be chosen to fulfill reactive power requirement. Even though the switched capacitor scheme is economical, it has the drawback of adjusting terminal voltage in steps. SVC which is a first-generation FACTS device requires considerable number of reactors and capacitors and has limited overload capacity [14]. STATCOM controls reactive power absorbed or injected into the power system using voltage source converters to regulate voltage and improve transient stability [15]. In RES based hybrid systems control of voltage and frequency poses a big challenge due to the intermittent nature of the sources. There are various voltage and frequency control schemes available in literature for isolated hybrid power systems [13-21]. Various energy control strategies for RES based hybrid systems have been given in [22-25] for its efficient performance. Some techniques have been given in literature where energy storage is used for frequency control [26-29] and load side converters or FACTS devices for control of reactive power [13], [16], [30-31]. With small scale hybrid systems, the problem of fluctuation of voltage and frequency occurs with change in load and/or change in input renewable source of energy hence simultaneous control of both parameters has been considered crucial [32]. Various techniques are used to find the parameters for optimal performance of the system [33-36]. The conventional technique Integral square error (ISE) criterion which has been shown to perform well in [37-39] has also been used in this study.

In the paper a coordinated active and reactive power control strategy of a hybrid system, operating in parallel with defined grid capacity, has been developed. Transfer function block diagram of the HSRE is developed from the real and reactive power balance equations for the individual components of the system. The model for defined grid operation as given in [32] is used in the system. The biogas generator set combines biogas engine model with synchronous generator along with IEEE type-I excitation model and AVR for voltage control [14] and electronic speed governor for frequency control [9], [40]. A novel mathematical model for the active and reactive power control of SCIG in the hybrid system has been derived. Voltage deviation signal is used for the model developed for STATCOM to remove any mismatch of reactive power in the system. The control system response has been optimized using ISE criterion. Small signal stability studies have been conducted of the developed model HSRE, with step disturbances in load active and reactive power as well as input wind speed, to prove the stability of the system.

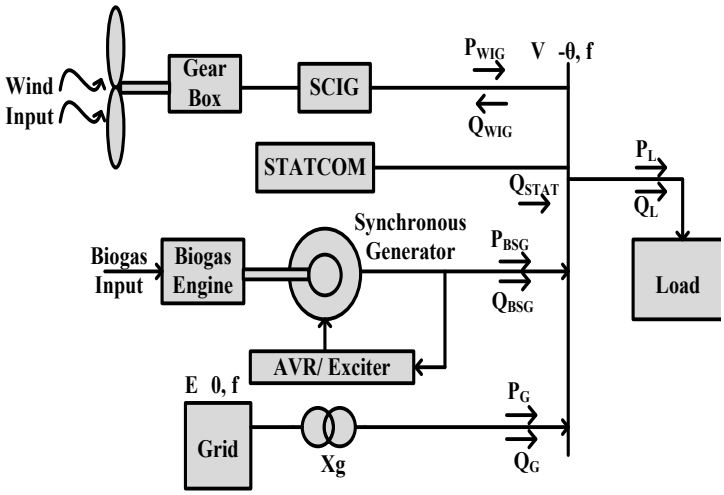

Fig. 1. Single line diagram of HSRE

2. Mathematical Modelling of the HSRE

The wind-biogas based HSRE comprising of synchronous generator, SCIG, electrical loads, control mechanism and STATCOM with defined grid supply is shown in Fig. 1. Active power requirement of the consumer load is met by SCIG of WECS and synchronous generator of biogas-genset. The reactive power needed by SCIG and load is supplied by synchronous generator and STATCOM. Grid does not participate in fulfilling the deviations in system load as well as change in input wind power. The real and reactive power balance equations of the HSRE at steady state are given by

$$P_{WIG} + P_{BSG} + P_G = P_L \tag{1}$$

$$Q_{BSG} + Q_{STAT} + Q_G = Q_L + Q_{WIG} \tag{2}$$

Post the disturbance in reactive power of load ΔQ_L, the system experiences a variation in voltage which leads to an incremental change in reactive power of other elements. The deviation of voltage ΔV resulted from net reactive power surplus ($\Delta Q_{BSG}+\Delta Q_{STAT}+\Delta Q_G-\Delta Q_{WIG}-\Delta Q_L$) in the system [13] is given by

$$\Delta V(s) = \frac{K_V}{1+sT_V}[\Delta Q_{BSG}(s) + \Delta Q_{STAT}(s) + \Delta Q_G(s) - \Delta Q_{WIG}(s) - \Delta Q_L(s)] \tag{3}$$

where, K_V is the gain constant and T_V is the time constant due to magnetizing reactance of the system generators. Similarly post disturbance in active power of load, ΔP_L the system experiences change in frequency which leads to real power surplus ($\Delta P_{BSG}+\Delta P_{WIG}+\Delta P_G-\Delta P_L$) which in turn will increase the frequency by ΔF and voltage angle by $\Delta\theta$. The deviation in frequency and voltage angle [32] is given as

$$\Delta F(s) = \frac{K_{FS}}{1+sT_{FS}}[\Delta P_{BSG}(s) + \Delta P_{WIG}(s) + \Delta P_G(s) - \Delta P_L(s)] \quad (4)$$

$$\Delta\theta(s) = [2\pi\Delta F(s)]/[s] \quad (5)$$

where K_{FS} and T_{FS} are the gain and time constants respectively of the HSRE.

2.1 Modeling of SCIG

The equivalent circuit of the squirrel cage induction generator is shown in Fig. 2. Small changes in active power generated by SCIG, ΔP_{WIG}, can be expressed in terms of V, generator data specifications and slip as given by

$$\Delta P_{WIG}(s) = K_{1W}\Delta V(s) + K_{2W}\Delta s(s) \quad (6)$$

where, $K_{1W} = (-2R_Y V)/(R_Y{}^2 + X_{EQ}{}^2)$ (7)

$$K_{2W} = [(V^2 + 2R_Y P_{IG})(R_2')]/[(R_Y{}^2 + X_{EQ}{}^2)*s^2] \quad (8)$$

Here, s is slip of the machine and X_m is the magnetizing reactance of the winding. The values of R_P, R_Y, R_2', X_{eq}, Req are given in Appendix A. Transfer function block diagram of the SCIG has been shown in Fig. 3. Similarly, the reactive power absorbed, ΔQ_{WIG} is expressed in terms of V, slip and generator specifications is given by

$$\Delta Q_{WIG}(s) = K_{3W}\Delta V(s) + K_{4W}\Delta s(s) \quad (9)$$

$$K_{3W} = -\frac{2X_{EQ}V}{R_Y{}^2 + X_{EQ}{}^2} \quad (10)$$

$$K_{4W} = \frac{2R_Y Q_{IG}}{R_Y{}^2 + X_{EQ}{}^2}\frac{R_2'}{s^2} \quad (11)$$

Since the SCIG consumes reactive power during its operation an additional source of reactive power generation like STATCOM has been used. It can absorb or generate reactive power using force commuted devices like IGBT, GTO etc. to control the reactive power flow through the grid in synchronization with the demand to stabilize voltage of the system. The configuration of the STATCOM has a coupling transformer, a voltage source converter(VSC) and a D.C. capacitor.

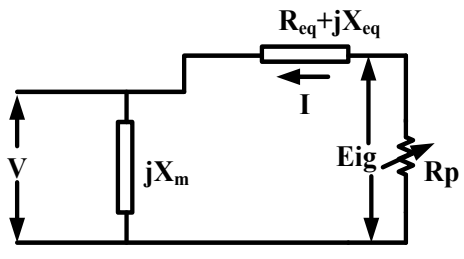

Fig. 2 Equivalent circuit of SCIG

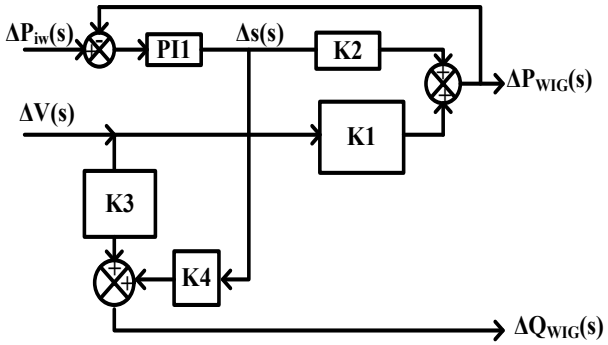

Fig. 3 Transfer function block diagram of SCIG

The magnitude of the fundamental component of the VSC is kV_{DC}, where V_{DC} is the voltage across the capacitor. α is STATCOM fundamental output voltage angle and B is the susceptance of the transformer. For modeling of the STATCOM [41] the reactive power injected to the bus is given by

$$Q_{STAT} = V^2 B - kV_{DC}BV\cos\alpha \quad (12)$$

Linearizing the above equation, we get:

$$\Delta Q_{STAT}(s) = K_{STAT1}\Delta\alpha(s) + K_{STAT2}\Delta V(s) \quad (13)$$

The values of K_{STAT1} and K_{STAT2} are given in Appendix B. The transfer function block diagram of STATCOM is shown in Fig.4.

2.2 Modelling of the Biogas-genset

The biogas-genset is fitted with automatic voltage regulator (AVR) and electronic speed governor for voltage and frequency control respectively. Model for small signal analysis of biogas-genset [32,40] is given by

$$\Delta P_B(s) = \frac{1}{1+sT_{B7}}\Delta X_{VB}(s) \quad (14)$$

$$\Delta Q_B(s) = K_{3B}\Delta E_{qB'}(s) + K_{4B}\Delta V(s) \quad (15)$$

Here, X_{VB} denotes the change in valve position which is tuned by the actuator upon receiving the signal given by the electronic speed governor as a reaction to the change in system frequency and voltage angle. For biogas genset IEEE type-I excitation control system, with saturation neglected, is used.

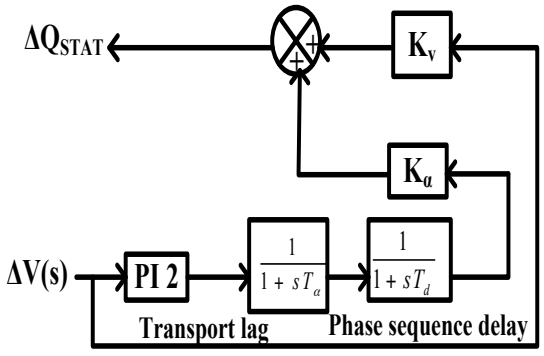

Fig. 4 Transfer function block diagram of STATCOM

The variation in reactive power, $\Delta Q_B'$ due to change in active power ΔP_B, while functioning at constant power factor is given by

$$\Delta Q'_B(s) = K_{RB}\Delta P_B(s) \quad (16)$$

The equations and values of K_{3B}, K_{4B} and K_{RB} are given in Appendix A and B.

2.3 Modeling of the Grid supply system:

The grid taken here as one of the feeder of a distribution substation which gives fixed supply of energy E, to a group of villages by day ahead load scheduling. In this case same amount of energy [E=reduced power (but fixed) *24 hours] will be taken from the grid over course of a day without any load shedding. The voltage on transformer primary side is taken as constant and voltage level of secondary winding is made equal to system bus voltage by the transformer. The small signal modeling of the grid supply system [32] is given by

$$\Delta P_G(s) = K_{1G}\Delta\theta(s) + K_{2G}\Delta V(s) \quad (17)$$

$$\Delta Q_G(s) = K_{3G}\Delta\theta(s) + K_{4G}\Delta V(s) \quad (18)$$

where, V and θ are the amplitude and angle of the system voltage respectively. The values of K_{1G}, K_{2G}, K_{3G} and K_{4G} are given in Appendix A.

2.4 Tuning of PI Controllers

The value of error *e(t)* produced due to difference between desired set point and measured value is continuously calculated by the PI Controller and a correction is applied based upon proportional and integral values (denoted as P, I respectively). It is denoted in mathematical forms as

$$u(t) = K_p e(t) + K_i \int_0^t e(t')dt' \quad (19)$$

where K_P, K_I are the coefficients of the proportional and integral terms respectively. ISE criterion has been chosen in the proposed system for tuning the PI controller gain settings. The error obtained is squared and integrated over the time in ISE. Due to consideration of square of errors it penalizes both positive and negative values of error. The ISE criterion is given as

$$\text{Min J} = \int_0^\infty (|e^2(t)|)dt \quad (20)$$

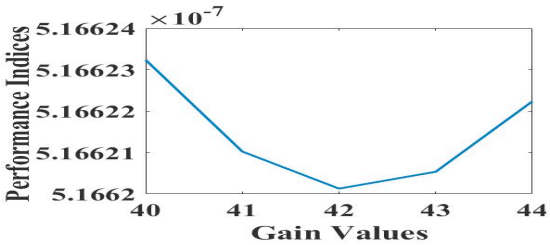

Fig. 5 Performance Index v/s Gain value curve for K_{P3} of PI-3 Controller

In this technique sequential optimization has been implemented where at a time one parameter is optimized while keeping other parameters constant using ISE criterion. For every parameter the process is repeated until the optimum value is obtained. The method is more suited where the number of parameters is less otherwise heuristic algorithms are preferred. The optimum value of controller's gain is chosen by finding the value of gain for which performance index J is minimum. ISE optimization criterion with reference to the HSRE is given as

$$\text{Min J} = \int_0^\infty (|\Delta\theta^2(t)| + |\Delta V^2(t)|)dt \quad (21)$$

Here, the performance index *J* signifies the area under the curve of error signal which has to be minimized. That gain value for which objective function gives a minima is the optimum gain setting of the controller. For illustration, the performance index curve obtained during the optimization problem has been shown in Fig. 5. It has been observed that the minimum value of performance index lies at the gain value of 42. Hence that value is chosen. And similarly rest of the gain values are optimized accordingly.

3. Simulation Results and Discussions

Simulation of the wind-biogas based HSRE was done by using values of the parameters given in Appendix B. The transfer function block diagram for the complete hybrid system is shown in Fig. 6. The gains K_P and K_I of the PI controllers used in the system are optimized using the conventional ISE criterion whose values are given in Table 1. The chosen sources- biogas, wind and grid of the hybrid system contribute to fulfill the load demand of 1 MW. Power supply contribution by the grid is taken as fixed 30% i.e. 300 kW and rest of the 70% of the demand is met by rest of the RES. The dynamic response of the HSRE for 1% step disturbance in load active and reactive power without any change in slip is shown in Fig. 7.

Table 1: Gain parameters of PI controllers of HSRE

Controller	Gain	ISE tuned gain value
PI 1	K_{P1}	-17.35
	K_{I1}	-103
PI 2	K_{P2}	-58.3
	K_{I2}	-42
PI 3	K_{P3}	-42
	K_{I3}	-91.5
PI 4	K_{P4}	-20
	K_{I4}	-212.5

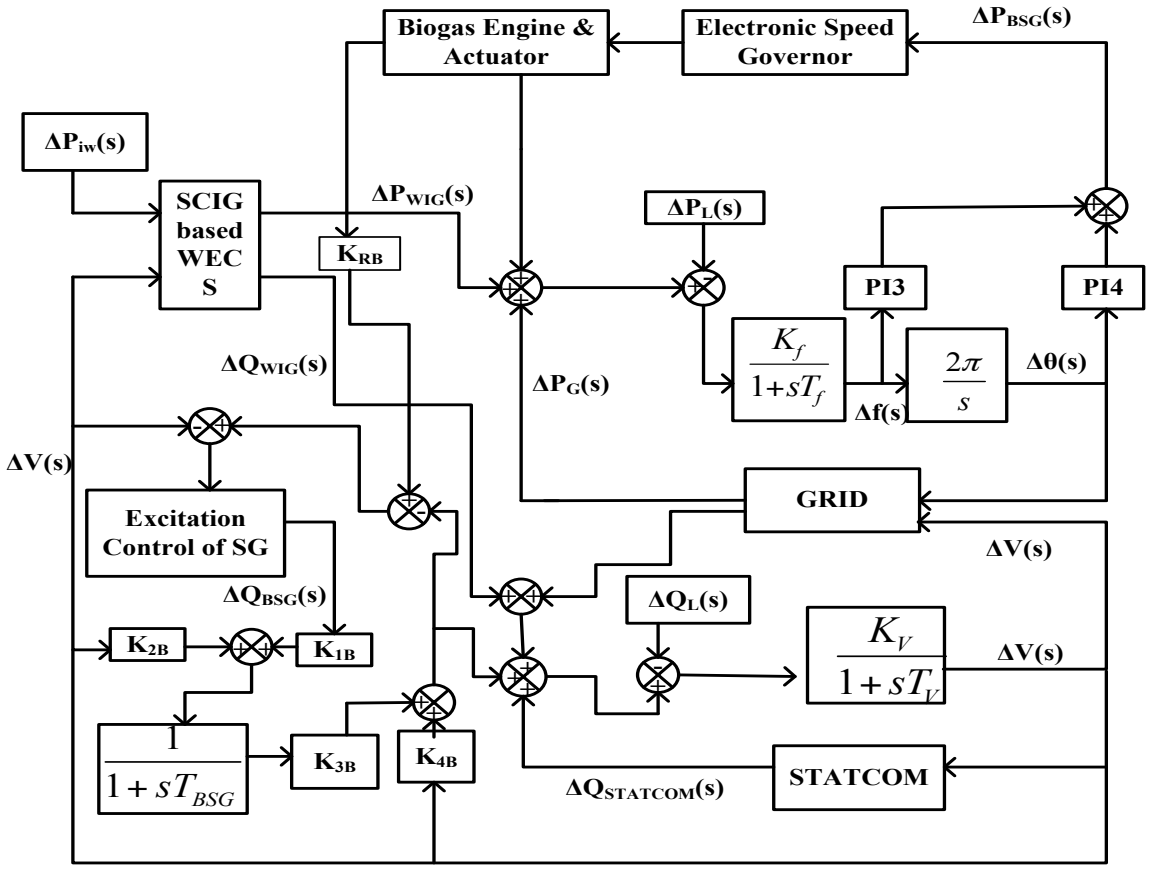

Fig. 6 Transfer function block diagram of hybrid system for rural electrification

As shown in Fig. 7(a) and Fig. 7(b) it has been observed that the change caused by the disturbance in the state variables Δf and Δθ settles within 2.16 seconds with no steady state error. It can be seen from Fig. 7(d) that due to no variation in input wind power there is no variation in wind active power output ΔP_w. Since the objective is to not draw any power from the grid to feed the disturbances hence ΔP_G=0 pu, as can be seen seen from Fig. 7(e). At steady state the active power change ΔP_L has been provided by the biogas genset when there is no variation in input wind power as shown in Fig. 7(f). At steady state the change in load reactive power ΔQ_L=0.01 pu and reactive power consumed by the wind, as seen from Fig.7(g), has been fulfilled by the biogas genset and the STATCOM, due to which the change in system voltage magnitude ΔV and grid reactive power, ΔQG is zero as can be seen from Fig. 7(c) and Fig. 7(h-j). Overall disturbance of reactive power of ΔQ_L=0.01 pu has been fulfilled by a combination of STATCOM and biogas given by total reactive power generated, ΔQ_T=0.01 pu as shown in Fig.7 (k). As can be observed from the plots, the voltage regulation is very fast whereas the reactive power control is very gradual since due to interactive control it has the effect of active power control dynamics as well. In this study change of reactive power along with variation in real power has been incorporated as shown in Fig.7 (f) and Fig. 7(i).

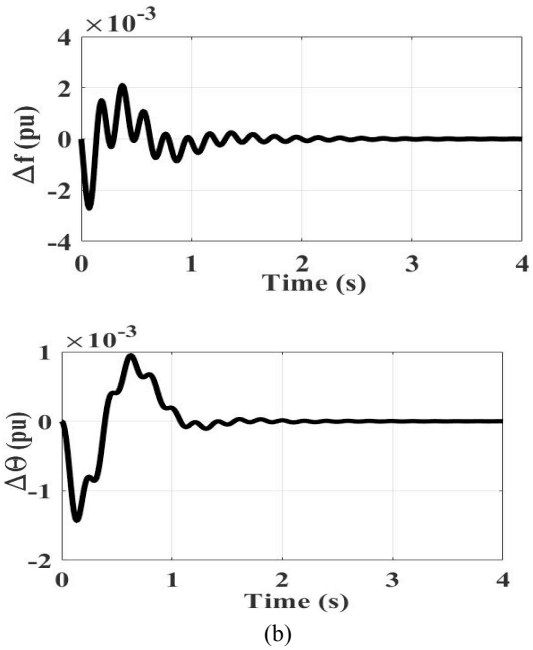

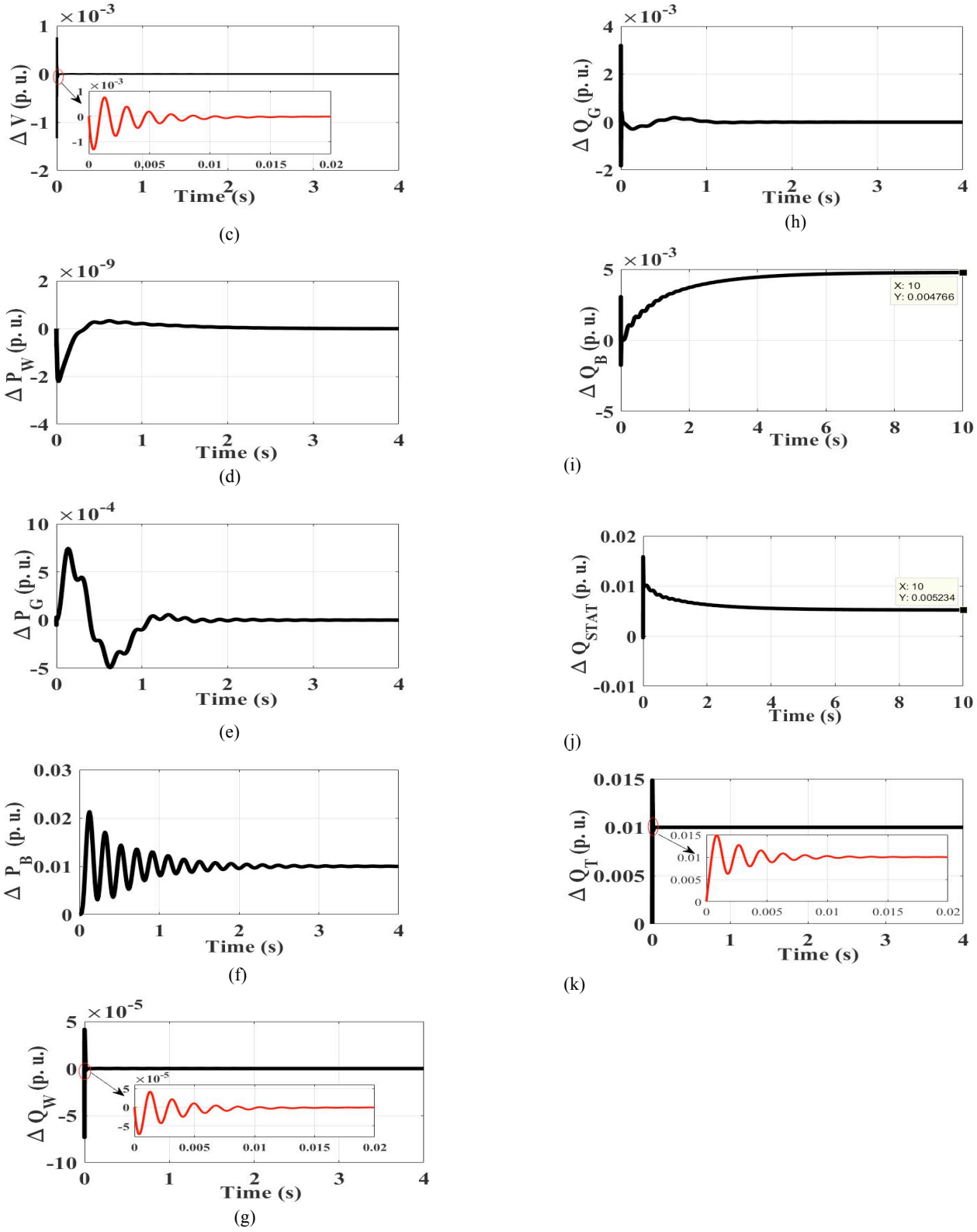

Fig. 7 Dynamic response of HSRE for 1% step disturbance in active and reactive power of consumer load and constant slip (a) Variation in frequency of system Δf (b) Variation in system voltage angle $\Delta\theta$ (c) Variation in system voltage magnitude , ΔV (d) Variation in active power of SCIG ΔP_{WIG} (e) Variation in active power of grid, ΔP_G (f) Variation in active power of biogas-genset ΔP_B (g) Variation in reactive power of SCIG, ΔQ_{WIG} (h) Variation in reactive power of grid, ΔQ_G (i) Variation in reactive power of biogas-genset, ΔQ_B (j) Variation in reactive power of STATCOM, ΔQ_{STAT} (k) Variation in total reactive power of system ΔQ_T.

Now, considering the case of variable slip where there is 1% step disturbance in input wind power along with the step disturbance in load active and reactive power and the dynamic responses are shown in Fig. 8. It can be examined from the results that change in system state variables Δf and Δθ settles in 2.16 seconds and 1.54 seconds respectively with no steady state error as shown in Fig.8(a) and Fig.8(b). This time the change in active power load

ΔP_L has been provided partially by the WECS, ΔP_w=0.01*K_W=0.00133 pu (where Kw is the participation factor of wind) and the remaining has been fulfilled by the biogas genset ΔP_B=.00867 pu at steady state as can be seen by Fig.8(d) and Fig.8(f), respectively. At steady state additional active power has not been drawn by the grid hence ΔP_G=0 as shown in Fig.8(e). The step disturbance in consumer load reactive power ΔQ_L=0.01 and reactive power consumed by wind turbine as shown in Fig.8(g) has been fulfilled by biogas genset and the STATCOM under steady state conditions as can be seen from Fig.8 (f) and Fig. 8(j). Hence the disturbance in the system voltage magnitude ΔV and grid reactive power ΔQ_G becomes zero as shown in Fig.8 (c) and Fig.8 (h). Even though the control of voltage is very fast, and the transients are removed in about 0.007s the overall control of reactive power is very gradual due to simultaneous control of active power.

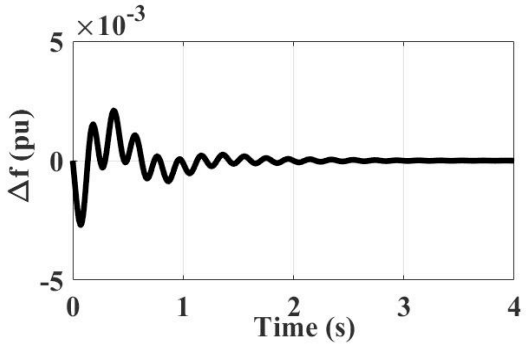

(a)

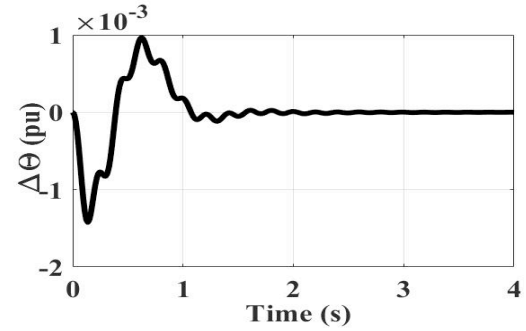

(b)

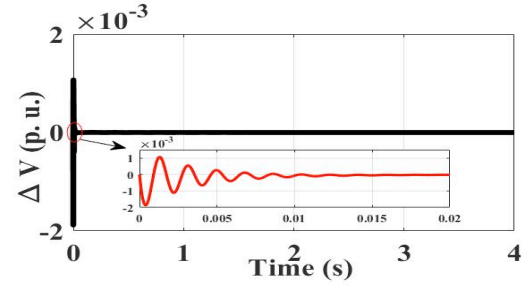

(c)

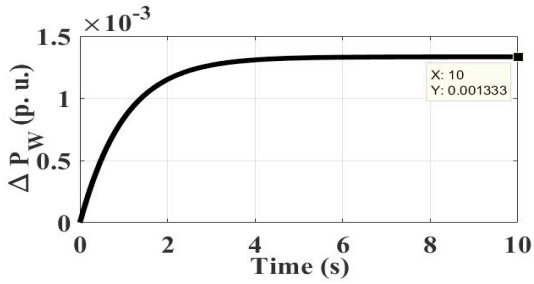

(d)

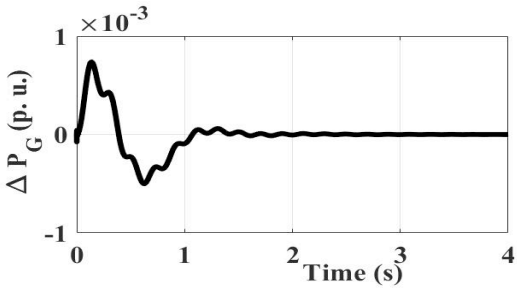

(e)

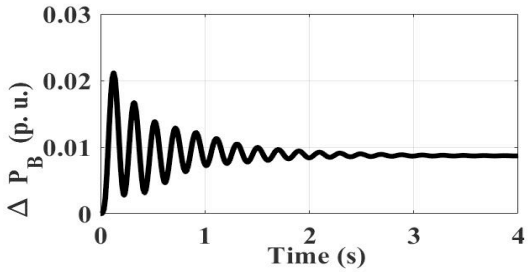

(f)

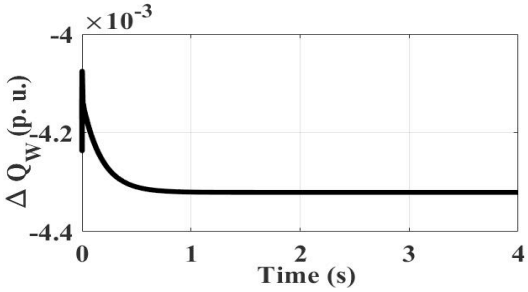

(g)

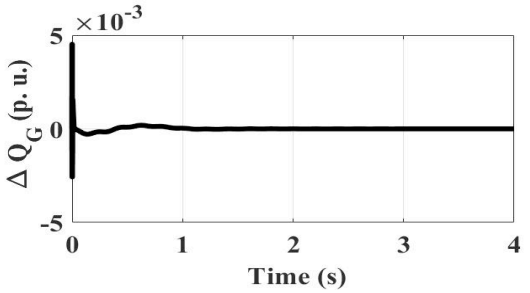

(h)

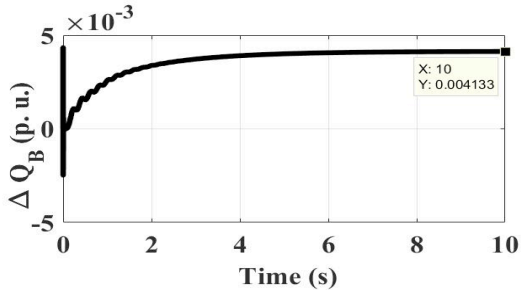

(i)

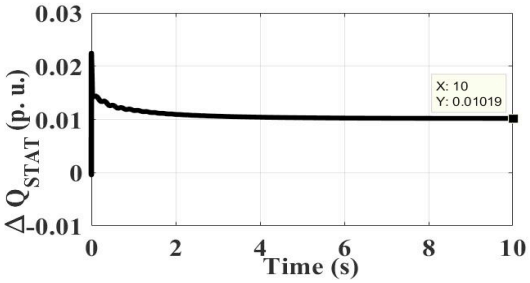

(j)

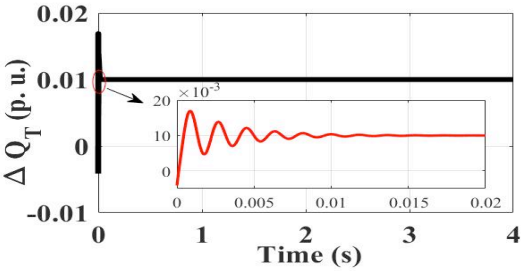

(k)

Fig.8 Dynamic response of HSRE for 1% step disturbance in load active and reactive power and variation in input wind speed (a) Change in frequency of system Δf (b) Change in system voltage angle $\Delta\theta$ (c) Change in voltage magnitude , ΔV (d) Change in active power of SCIG ΔP_W (e) Change in active power of grid, ΔPg (f) Change in active power of biogas-genset ΔP_B (g) Change in reactive power of SCIG, ΔQw (h) Change in reactive power of grid, ΔQ_G (i) Change in reactive power of biogas-genset, ΔQ_B (j) Change in reactive power of STATCOM, ΔQ_{STAT} (k) Change in total reactive power of system ΔQ_T

Conclusion

The model has been developed for active and reactive power control of HSRE. The dynamic performance of HSRE has been studied under step disturbances in system load as well as input wind power. It is demonstrated through the results that power balance is maintained between individual components of the system. After disturbance in system load and input wind power the grid goes back to feeding its defined share of 30% at steady state. The results also show that at steady state imbalance in load active power and/or variation in input wind power is handled by complementary variation in active power generated by the biogas-genset. The overall reactive power control turns out to be slow due to simultaneous active power control dynamics involved in the control strategy. STATCOM has been shown to fulfill the reactive power requirement of the load as well as SCIG under steady state conditions and the demand is initially met by the synchronous generator. Decoupled control hasn't been considered since the size of the hybrid system is small and the variations in frequency and voltage occur with load disturbance and input wind power disturbances. Hence coordinated control of voltage and frequency has been considered in this paper. As required the changes in load active and reactive power are not met by the grid and the system is stable for variations in load as well as input wind power. The model has been simulated only for small signal disturbances and can be extended by adding sources such as solar PV, small hydro available at specific sites so that according to availability of the resource proposed model can be implemented.

References

[1] "World Bank Annual report," 2014. [www.worldbank.org].

[2] "Ministry of Power, Rural electrification Annual Report," 2016. [www.powermin.nic.in].

[3] "World Bank Report: Empowering rural India-Expanding access by mobilizing local resources," 2010. [www.worldbank.org].

[4] James Cust, Anoop Singh and Neuhoff Karsten, "Rural electrification in India: Economic and industrial aspect of renewables"," pp. 1-36, 2007.

[5] H. Nacfaire, Wind-Diesel and wind autonomous energy systems, London: Elsevier Applied Science, 1989.

[6] Benjamin Kroposki , "Integrating high levels of variable renewable energy into electric power systems," *Journal of Modern Power Systems and Clean Energy,* pp. 831-837, November 2017.

[7] M. H. Nehrir, C. Wang, K. Strunz, H. Aki, R. Ramakumar, J.Bing and et.al., "A Review of Hybrid Renewable/Alternative energy systems for electric power generation: configurations,control and

applications," *IEEE Transactions on Sustainable Energy,* vol. 2, no. 4, 2011.

[8] P.Balamurugan, S. Kumaravel and T. Jose, "Optimal Operation of biomass/wind/PV hybrid energy system for rural areas," *International Journal of Green Energy,* pp. 104-116, 2009.

[9] L.Wang and P.Lin, "Analysis of a commercial biogas generation system using a gas engine-induction generator set," *IEEE Transactions on Energy Conversion,* vol. 24, pp. 230-239, March 2009.

[10] N.Kumaresan, "Analysis and control of three-phase self-excited induction generators supplying single-phase AC and DC loads," *IEE Proceedings - Electric Power Applications,* vol. 152, pp. 739-747, May 2005.

[11] Devashish and A. Thakur, "A Comprehensive Review on Wind Energy System for Electric Power Generation: Current Situation and Improved Technologies to Realize Future Development," *International Journal of Renewable Energy Research-IJRER,* vol. 7, no. 4, 2017.

[12] R.C.Bansal, T.S.Bhatti and D.P.Kothari, "A bibliographical survey on induction generators for application of non-conventional energy systems," *IEEE Trans. Energy Conversion,* vol. 18, pp. 433-439, 2003.

[13] Pawan Sharma and T.S.Bhatti, "Performance Investigation of Isolated Wind–Diesel Hybrid Power Systems With WECS Having PMIG," *IEEE Transactions on Industrial Electronics,* vol. 60, pp. 1630-1637, April 2013.

[14] R.C.Bansal, "Automatic reactive power control of autonomous hybrid power system," Delhi, India, 2002.

[15] M. Yesilbudak, S. Ermis and R. Bayindir, "Investigation of the effects of FACTS devices on the voltage stability of power systems," in *2017 IEEE 6th International Conference on Renewable Energy Research and Applications (ICRERA)*, San Diego, CA, 2017.

[16] R.C.Bansal, T.S.Bhatti and D.P.Kothari, "A Novel Mathematical Modelling of Induction Generator for Reactive Power Control of Isolated," *Internal Journal of Modelling and Simulation,* 2004.

[17] D.K.Yadav and T.S.Bhatti, "Voltage control through reactive power support for WECS based hybrid power system," *International Journal of Electrical Power & Energy Systems,* vol. 62, pp. 507-518, November 2014.

[18] H.Wen, H.Yu and Y.Hu,"Modeling and analysis of coordinated control strategies in AC microgrid," in *2016 IEEE International Conference on Renewable Energy Research and Applications(ICRERA)*,Birmingham, 2016.

[19] A. M. Kassem and A. Y. Abdelaziz, "Reactive power control for voltage stability of standalone hybrid wind–diesel power system based on functional model predictive control," *IET Renewable Power Generation,* vol. 8, pp. 887-899, 2014.

[20] D. J. Lee and L. Wang, "Small-Signal Stability Analysis of an Autonomous Hybrid Renewable Energy Power Generation/Energy Storage System Part I: Time-Domain Simulations," *IEEE Transactions on Energy Conversion,* vol. 23, pp. 311-320.

[21] A. M. O. Haruni, M. Negnevitsky, M. E. Haque and A. Gargoom, "A Novel Operation and Control Strategy for a Standalone Hybrid Renewable Power System," *IEEE Transactions on Sustainable Energy,* vol. vol. 4, no. 2, pp. 402-413, 2013.

[22] Yousef Allahvirdizadeh, Mustafa Mohamadian and Mahmoud-Reza HaghiFa, "A Comparative Study of Energy Control Strategies for a Standalone PV/WT/FC Hybrid Renewable System," *International Journal of Renewable Energy Research-IJRER,* vol. 7, no. 3, 2017.

[23] J. Choi, W. K. Park and I. W. Lee, "Application of vanadium redox flow battery to grid connected microgrid energy management," in *2016 IEEE International Conference on Renewable Energy Research and Applications (ICRERA)*, Birmingham, 2016

[24] S. M. Vaca, C. Patsios and P. Taylor, "Enhancing frequency response of wind farms using hybrid energy storage systems," in *2016 IEEE International Conference on Renewable Energy Research and Applications (ICRERA)*, Birmingham, 2016.

[25] Alfonso Damiano, Gianluca Gatto, Ignazio Marongiu, Mario Porru and Alessandro Serpi, "Real-Time Control Strategy of Energy Storage," *IEEE Transactions on sustainable Energy,* vol. 5, no. 2, 2014.

[26] H. Turker and P. Favre-Perrod, "Management, optimal sizing and technical-economic analysis of batteries for constant production in photovoltaic systems," in *2016 IEEE International Conference on Renewable Energy Research and Applications (ICRERA)*, Birmingham, 2016

[27] Swaminathan Ganesan, Ramesh V and Umashankar S, "Hybrid Control of Microgrid with PV, Diesel Generator and BESS," *International Journal of Renewable Energy Research-IJRER,* vol. 7, no. 3, 2017.

[28] S. Vachirasricirikul and I. Ngamroo, "Robust LFC in a Smart Grid With Wind Power Penetration by Coordinated V2G Control and Frequency Controller,"

IEEE Transactions on Smart Grid, vol. 5, Jan 2014.

[29] Q. Xu, J. Xiao, P. Wang, X. Pan and C. Wen, "A Decentralized Control Strategy for Autonomous Transient Power Sharing and State-of-Charge Recovery in Hybrid Energy Storage Systems," *IEEE Transactions on Sustainable Energy,* vol. 8, no. 4, pp. 1443-1452, 2017.

[30] R. Aghatehrani, L. Fan and R. Kavasseri, "Coordinated reactive power control of DFIG rotor and grid sides converters," in *2009 IEEE Power & Energy Society General Meeting*, Calgary, AB, 2009.

[31] G. S. Kaloi, J. Wang and M. HussainBaloch, "Active and reactive power control of the doubly fed induction generator based on wind energy conversion system," *Energy Reports,* vol. 2, pp. 194-200, 2016.

[32] D.K.Yadav, T.S.Bhatti and Ashu Verma, "Study of Integrated Rural Electrification System Using Wind-Biogas Based Hybrid System and Limited Grid Supply System," *International Journal of Renewable Energy Research-IJRER,* vol. 7, 2017.

[33] Mohamed Nadour, Ahmed Essadki and Tamou Nasser, "Comparative Analysis between PI & Backstepping Control Strategies of DFIG Driven by Wind Turbine," *International Journal of Renewable Energy Research-IJRER,* vol. 7, no. 3, 2017.

[34] K.A.G.Rao, B.A.Reddy and P.D.Bhavani, "Fuzzy PI and integrating type fuzzy PID controllers of linear, nonlinear and time delay systems," *International Journal of Computer Applications,* vol. 1, pp. 41-47, 2010.

[35] S.M.Giriraj, D.Jayaraj and A.R.Kishan, "PSO based tuning of a PID controller for a high performance drilling machine," *Innternational Journal of Computer Apllications,* vol. 1, no. 19, pp. 12-18, 2010.

[36] Jizhen Liu, Jizhen Liu, Tongwen Chen and Horacio J.Marquez, "Comparison of some well-known PID tuning formulas," *Computers and Chemical Engineering,* vol. 30, no. 9, 2006.

[37] Y.K.Soni and R.Bhatt, "Simulated annelaing optimized PID controller design using ISE,IAE,IATE and MSE error criterion," *International Journal of Advanced Research in Computer Engineering and Technology,* vol. 2, pp. 2337-2340, 2013.

[38] K. Mohamed Hussain, R. Allwyn Rajendran Zepherin, ,M. Shantha and S.M. Giriraj Kumar, "Comparison of PID Controller Tuning Methods with Genetic Algorithm for FOPTD System," *Int. Journal of Engineering Research and Applications,* vol. 4, pp. 308-314, 2014.

[39] N. Pathak, A. Verma and T. S. Bhatti, "New optimization criterion for load frequency control of power system," in *IEEE 1st International Conference on Power Electronics, Intelligent Control and Energy Systems (ICPEICES)*, Delhi, 2016.

[40] K. E. Yeager and J. R. Willis, "Modeling of emergency diesel generators in an 800 megawatt nuclear power plant," *IEEE Transactions on Energy Conversion,* vol. 8, no. 3, pp. 433-441, 1993.

[41] B. Kouadri and Y.Tahir, "Power flow and transient stability modeling of a 12-Pulse," *Journal of Cybernetic and Informatics,* 2008.

Appendix A

The constants K_{1G}, K_{2G}, K_{3G}, K_{4G} of Equations (17) & (18) are given as:

$$K_{1G} = \frac{E_G V \cos\theta}{X_G} \quad \text{A.1}$$

$$K_{2G} = \frac{E_G \sin\theta}{X_G} \quad \text{A.2}$$

$$K_{3G} = \frac{E_G \sin\theta}{X_G} \quad \text{A.3}$$

$$K_{4G} = \frac{E_G \cos\theta - 2V}{X_G} \quad \text{A.4}$$

$\Delta X_{VB}(s)$ from equation (14) is given as:

$$\Delta X_{AB}(s) = \frac{(1+sT_{B3})}{1+sT_{B1}+s^2T_{B1}T_{B2}} \quad \text{A.5}$$

Change in actuator will further depend upon electronic speed governor design and is given by

$$\Delta X_{VB}(s) = \frac{(1+sT_{B4})}{s(1+sT_{B5})(1+sT_{B6})}\Delta X_{AB}(s) \quad \text{A.6}$$

The small deviation in voltage behind transient reactance, $\Delta E'qb(s)$[13,16,25] is given by:

$$(1+sT_{GB})\Delta E'_{qB}(s) = [K_{1B}\Delta E_{fdB}(s) + K_{2B}\Delta V(s)] \quad \text{A.7}$$

$$K_{1B} = \frac{X_{dB}'}{X_{dB}} \quad \text{A.8}$$

$$K_{2B} = \frac{(X_{dB} - X_{dB}')\cos(\delta+\theta)}{X_{dB}} \quad \text{A.9}$$

$$K_{3B} = \frac{V\cos(\delta+\theta)}{X'_{dB}} \quad \text{A.10}$$

$$K_{4B} = \frac{E_{qB}'\cos(\delta+\theta) - 2V}{X_{dB}'} \quad \text{A.11}$$

$$K_{RB} = \frac{\sqrt{(1-pf_b^2)}}{pf_b} \quad \text{A.12}$$

For SCIG

$$R_{eq} = R_1 + R_2' \quad \text{A.13}$$

$$R_P = \frac{R_2'(1-s)}{s} \quad \text{A.14}$$

$$R_Y = R_P + R_{EQ} \quad \text{A.15}$$

$$X_{eq} = X_1 + X_2 \quad \text{A.16}$$

$$K_{STAT1} = kV_{DC}BV\sin\alpha \quad \text{A.17}$$

$$K_{STAT2} = 2VB - kV_{DC}B\cos\alpha \quad \text{A.18}$$

where, R_1, R_2 are the stator and rotor side resistance and X_1, X_2 are the stator and rotor side reactance.

Appendix B

Table 2: Capacity of the System

Sources	Generation $P_G^0=P_L$ (kW)	Rated Capacity (kW)
Grid	300	350
Wind	200	400
Biogas	500	750
Total	1000	1500

Table 3 System data

Parameters	Values
Number of villages	4
Number of houses per village	1600
Domestic electric demand per	1 kW
Total domestic demand	1600 kW=1.6 MW
Number of irrigation pumps per	10
Total number of irrigation pumps	40
Size/rating of each pump	5 kW
Total load by irrigation pumps	200 kW
Total load demand for other	20 kW
Total contract demand for 4	1820 kW
Maximum diversified demand	1820*0.55=1000
Nominal load of the system	1000 kW
Nominal frequency of the system	50 Hz

Gain and Time constant of the system: K_f= 75 Hz/pu kW; T_f=15s

Reactive power gain constants of the system

K_V= 1.5 pu kV/pu kVAR T_V= 0.00212 s

Grid

P_G=0.2; Q_G=.09686; K_{1G}=-2.8746; K_{2G}=0.2; K_{3G}=0.2

K_{4G}=-2.6809

Wind

P_W=0.13335 pu kW Q_W=0.24169 pu kVAR

K_{1W}=0.0889; K_{2W}=-1.267; K_{3W}= -0.0184; K_{4W}=0.5474; s= -0.0333

Biogas

P_B=.33335; Q_B=.16145; X_d=1.0 pu; Xd'=0.15 pu; T_{do}'=5s T_B=0.75s; K_{1B}=0.15; K_{2B}=.84326; K_{3B}=2.45; K_{4B}=-2.308 T_{B1}=0.01s; T_{B2}=0.02s; T_{B3}=0.15s; T_{B4}=0.2s;T_{B5}=0.014s; T_{B6}=0.04s; T_{B7}=0.036s; K_{AB}=200; T_{AB}=0.05s; K_{EB}=1; T_{EB}=2s; K_{FB}=0.5 ; T_{FB}=1s; Reactive power participation factor: K_{RB}=0.48432

STATCOM: K_{STAT1}= 0.79944 K_{STAT2} = 0.730794